analytical chemistry

Article

pubs.acs.org/ac

Detection of Single-Nucleotide Polymorphisms Using an ON−OFF Switching of Regenerated Biosensor Based on a Locked Nucleic Acid-Integrated and Toehold-Mediated Strand Displacement Reaction

Zhong Feng Gao, Yu Ling, Lu Lu, Ning Yu Chen, Hong Qun Luo, and Nian Bing Li*

Key Laboratory of Eco-environments in Three Gorges Reservoir Region (Ministry of Education), School of Chemistry and Chemical Engineering, Southwest University, 2, Tiansheng Road, BeiBei District, Chongqing 400715, P.R. China

Supporting Information

ABSTRACT: Although various strategies have been reported for single-nucleotide polymorphisms (SNPs) detection, development of a time-saving, specific, and regenerated electrochemical sensing platform still remains a realistic goal. In this study, an ON−OFF switching of a regenerated biosensor based on a locked nucleic acid (LNA)-integrated and toehold-mediated strand displacement reaction technique is constructed for detection of SNPs. The LNA-integrated and methylene blue-labeled capture probe with an external toehold is designed to switch on the sensing system. The mutant-type DNA probe completes complementary with the capture probe to trigger the strand displacement reaction, which switches off the sensing system. However, when the single-base mismatched wild-type DNA probe is presented, the strand displacement reaction cannot be achieved; therefore, the sensing system still keeps the ON state. This DNA sensor is stable over five reuses. We further testify that the LNA-integrated sequence has better recognition ability for SNPs detection compared to the DNA-integrated sequence. Moreover, this DNA senor exhibits a remarkable discrimination capability of SNPs among abundant wild-type targets and 6000-fold (*m*/*m*) excess of genomic DNA. In addition, it is selective enough in complex and contaminant-ridden samples, such as human urine, soil, saliva, and beer. Overall, these results demonstrate that this reliable DNA sensor is easy to be fabricated, simple to operate, and stable enough to be readily regenerated.

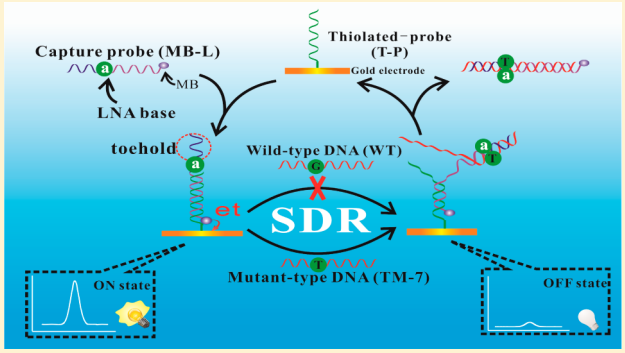

Single-nucleotide polymorphisms (SNPs) are the most common form of genetic variation in human genes, which are closely associated with various phenotypes and genetic diseases.[1,2] Highly selective and sensitive detection methods for SNPs are essential in clinical diagnosis and research uses.[3,4] Currently, the reported SNPs discrimination methods can be mainly categorized into two groups, namely, enzyme-assisted discrimination and specific hybridization-based methods.[5,6] Enzyme-assisted discrimination has been widely used, such as endonuclease,[7,8] ligation chain reaction,[9−11] and rolling circle amplification.[12,13] However, the inherent drawbacks such as unstable activity of enzyme and rigorous experimental conditions limit its applications in biosensors. It is desired to develop a sensitive and selective enzyme-free method to meet specific needs for SNPs detection. The other strategy, a hybridization-based method, has high sensitivity and is able to discriminate the difference between perfectly matched and single-nucleotide mismatched targets.[14−16] In addition, the simplicity and straightforwardness of a hybridization-based method provides the possibility of detecting SNPs genotyping of real samples.[17]

Recently, the strand displacement reaction (SDR) has been explored as a powerful strategy to control and construct DNA hybridization.[18−20] Toehold is a short, single-stranded, and overhang region, typically consisting of 5−8 nucleotides (nt).[18] Hybridization is initiated by the exposed toehold, leading to a branch migration process that displaces another strand from the substrate. In addition, the rate of the strand exchange reaction can be enhanced by a factor of 10^6 using toehold-mediated SDR.[21] A variety of SNPs genotyping methods have been developed based on toehold-mediated SDR, such as fluorescence microscopy,[22] quartz crystal microbalance,[6] and atomic force microscope imaging.[23] However, these methods still have some limitations, such as being time consuming and having high cost. It is necessary to develop a highly sensitive and simple method to meet the specific need for SNPs detection based on toehold-mediated SDR.

Locked nucleic acid (LNA) has attracted considerable attention in recent years due to its unique structure.[24−28] LNA is a conformationally restricted ribonucleotide analogue containing a methylene linkage between the 2′-O atom and the 4′-C atom of the ribose ring.[29,30] The constraint on the sugar

Received: November 9, 2013
Accepted: February 6, 2014
Published: February 6, 2014

   dx.doi.org/10.1021/ac500362z | *Anal. Chem.* 2014, 86, 2543−2548

moiety results in higher affinity and a higher melting temperature (T_m) value for the nucleic acid duplex.[31] It is noteworthy that the T_m reduction (ΔT_m) for the mismatch-bearing LNA/DNA hybrids is much greater than that of DNA/DNA hybrids according to theoretical calculations by Kurita et al.[32] The unique structural features make LNA an ideal research tool for SNPs detection.

Although strand displacement reaction and LNA-integrated probes techniques for detection of target DNA have achieved impressive results,[6,22,29] these methods are generally cumbersome and unreusable, and thus, development of a generally regenerated sensing platform for rapid detection of such targets remains a compelling goal. Here we report a reusable DNA sensor to detect SNPs, combining the features of enzyme-free, LNA-integrated, and toehold-mediated SDR techniques in an ON−OFF manner for the first time. The target sequence used in this study is a part of codon 273 mutation in the p53 tumor suppressor gene, which is a site-specific mutation of cytosine to thymine. This DNA sensor is easily fabricated and readily regenerated and functional even in contaminant-ridden samples, such as human urine, soil, saliva, and beer.

EXPERIMENTAL SECTION

Materials and Apparatus. Tris(2-carbozyethyl)phosphine hydrochloride (TCEP), 6-mercaptohexanol (MCH), and 2-amino-2-(hydroxymethyl)-1,3-propanediol (tris) were purchased from Aladdin Chemistry Co., Ltd. (Shanghai, China) and used without further purification. Other reagents of analytical reagent grade were purchased from Chengdu Kelong Chemical Reagents Factory (China) and used as received. Shancheng beer was purchased from a local supermarket (Chongqing, China). The buffer solution involved in this study was 20 mM Tris-HCl buffer (100 mM NaCl, pH 7.4). All solutions were prepared with Milli-Q water (18.2 MΩ cm) from a Milli-Q water system. The experiment temperature was kept with a SD-101-005DB super digital thermostat bath (Sida Experimental Equipment Ltd., Chongqing, China). DNA oligonucleotides were synthesized by Sangon Inc., Shanghai, China. Denatured herring sperm genomic DNA was purchased from Sangon Inc., Shanghai, China. All DNA sequences are listed in Table S1 (Supporting Information). A thiolated DNA probe was activated with 10 mM TCEP and stored in the dark at 4 °C for 2 h. All DNA samples were prepared by dissolving in 20 mM Tris-HCl solution (100 mM NaCl, pH 7.4).

Electrode Preparation and Electrochemical Measurements. The immobilized modified sensor was fabricated using gold electrodes (2 mm diameter, CHI Co., Ltd., Shanghai, China). Electrodes were prepared using our previous method.[33] In brief, the gold electrode was carefully polished for 3 min using alumina powder (0.3 μm) and followed by polishing for 10 min using 0.05 μm alumina powder. After that, the polished electrode was rinsed with ultrapure water thoroughly and sonicated in ultrapure water, ethanol, and ultrapure water for each 3 min to remove the remaining alumina powder on gold surface. Then, the gold electrode was electrochemically cleaned in 0.5 M H_2SO_4 using cyclic voltammetry in the range from −0.3 to 1.6 V at a scan rate of 0.1 V/s for 25 cycles and finally dried with nitrogen.

Alternating Current Voltammetric Measurement Procedure. Alternating current voltammetry (ACV) was carried out on a CHI660B electrochemical station (Chenhua Instruments Co., Shanghai, China) in a conventional three-electrode cell with a gold working electrode, a platinum counter electrode, and an Ag/AgCl reference electrode. In addition, the cell was enclosed in a grounded Faraday cage. ACV scan from −0.5 to 0 V was performed in phosphate-buffered (PB) (100 mM phosphate, pH 7.4) solution with a step potential of 5 mV, amplitude of 25 mV, and frequency of 10 Hz. All measurements were obtained after the electrode was immersed in PB solution for 10 min.

The thiolated DNA (T-P) solution (100 nM) was dropped on the surface of polished gold electrode for 12 h at 25 °C of hybridization. Then, the electrode was dipped into 2 mM MCH solution for 1 h to minimize the nonspecific adsorption. Next, the gold surface was immersed in 100 nM LNA-integrated capture probe solution (MB-L) to hybridize for 40 min. Then, ACV measurement was performed in PB solution. Afterward, 100 nM mutant-type target DNA (TM-7) or wild-type DNA (WT) was dropped onto the gold surface. After hybridization for 20 min at 45 °C, the strand displacement reaction was finished and ACV measurement was conducted again. The released T-P-modified electrode can be used to start another round of detection.

Selectivity and Specificity Measurement. After the T-P/MB-L hybrids formed, selectivity was assessed by incubating the electrode for 20 min at 45 °C in human urine or saliva (both collected, diluted 50% with the buffer solution, and used within 20 min), soil (soil stock solution was prepared by diluting 400 mg of soil to a final volume of 1 mL with the buffer solution), or beer (Shancheng beer was diluted 50% with the buffer solution). In addition, specificity was assessed by incubating the electrode for 20 min at 45 °C in the presence of TM-7/WT mixture or excess genomic DNA sample. The genomic DNA sample was prepared as follows: 0.2 mg/mL denatured herring sperm genomic DNA was spiked with 32 ng (100 nM) of TM-7. Then, ACV measurement was performed in PB solution. Each experiment was conducted using three independent electrodes.

Melting Temperature Measurement. Melting curves of MB-L/TM-7, MB-L/WT, MB-D/TM-7, and MB-D/WT duplexes were carried out using a circular dichroism spectrometer (Applied Photophysics Ltd., UK). The experiment was conducted in a 20 mM Tris-HCl buffer (100 mM NaCl, pH 7.4), and the final concentration of each DNA sample was 1 μM. DNA samples were denatured at 90 °C for 5 min and slowly cooled to room temperature. Absorbance at 260 nm was recorded from 30 to 90 °C with a 2 °C increase per minute.

RESULTS AND DISCUSSION

Reaction Mechanism of Regenerated Biosensor. The DNA sensor architecture and signaling mechanism are depicted in Scheme 1. The fabrication process of the sensor involves immobilization of a thiolated DNA probe (T-P) onto gold surface. The capture probe is methylene blue labeled and LNA integrated (MB-L), containing a toehold-mediated region. We design the mismatched site, modified with LNA base, at the inner end of toehold region, which possesses the highest discrimination ability as reported.[6,22] Alternating current voltammetry has been conducted to evaluate the sensor performance. Upon introduction of MB-L, the peak current is enhanced by formation of MB-L/T-P hybrids, because the MB tag is close to the gold surface to allow electron transfer. Thus, the system presents the ON state. The exposed overhang initiates a strand displacement reaction in the presence of a mutant-type target DNA molecule (TM-7). In the process of

dx.doi.org/10.1021/ac500362z | Anal. Chem. 2014, 86, 2543−2548

Scheme 1. Schematic Representation of Regenerated DNA Biosensor Architecture and ON−OFF Switching Signaling Principle for SNPs Detection[a]

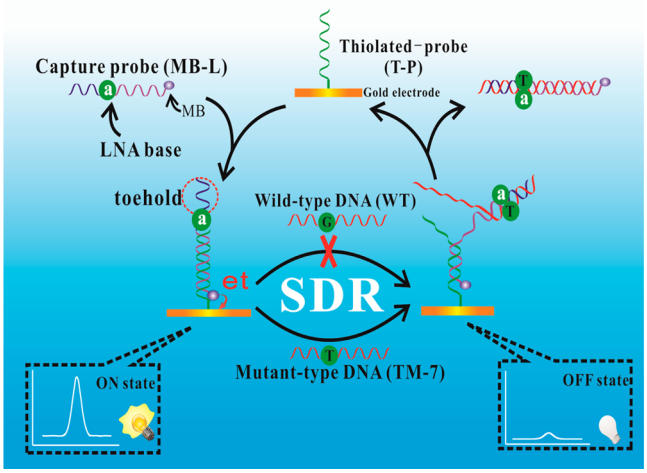

[a]The symbol "SDR" means strand displacement reaction.

hybridization with TM-7, T-P is released, leaving MB-L/TM-7 hybrids in solution. Thus, the peak current is reduced, and the system presents the OFF state. The released T-P can be used to bind another MB-L to start another round of target recycling-oriented reaction. Thus, consecutive reversible ON−OFF switching is established. However, the displacement process is prevented in the presence of the wild-type target (WT), because the single-base mismatch causes inhibition of hybridization between MB-L and WT. Thus, the peak current still stays at high level (ON state). On the basis of the phenomena mentioned above, a difference of current can be measured, which offers specific discrimination for SNPs detection.

Feasibility Tests of Discrimination for Single-Nucleotide Polymorphisms. As can be seen in Figure 1, a sharp and well-defined peak current appeared due to formation of MB-L/T-P hybrids (curve a). After addition of TM-7 solution in a T-P/MB-L hybrids system, a nearly 91.6% decrease in current was observed (curve b), revealing a strong affinity of MB-L to target DNA. However, when the single-base mismatched wild-type DNA was presented, the current signal hardly changed (curve c), indicating that the LNA-integrated sequence has a strong discrimination ability for a single-base mismatched sequence. To further validate the strong affinity of LNA, we chose the pure DNA-integrated sequence (MB-D) as the capture probe. As shown in Figure 1, the current generated was only about 72.5% of that by MB-L at the same condition (curve d), and only a 69.6% signal decrease was obtained after the SDR completed (curve e), implying that the affinity of DNA is not as strong as that of LNA. Of note, nearly 33% signal change was observed (curve f) when the single-base mismatched wild-type DNA was added in the sensing system. This result further demonstrates that the LNA-integrated sequence has better recognition ability for SNPs detection than the DNA-integrated sequence does.

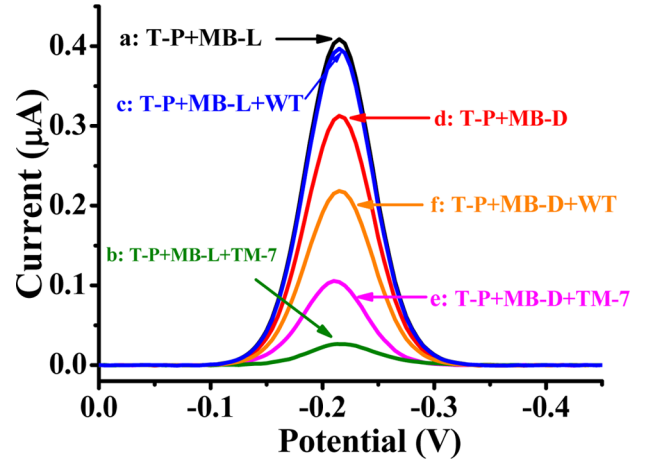

Figure 1. Alternating current voltammograms of the sensor. Each concentration of DNA probe used in the assay is 100 nM. Data shown are average measurements from three different electrodes. All measurements were performed in PB solution (100 mM phosphate, pH 7.4).

Optimum Conditions for the System. A series of experiments was performed to optimize the conditions for the system.

Influence of Incubation Time between T-P and MB-L. In order to obtain the optimal experimental condition, the hybridization time between T-P and MB-L was optimized by ACV measurement at various time points (Figure S1, Supporting Information). After measurements, the peak current at each time point was recorded. We note that the current rapidly increases with increasing hybridization time up to 40 min and then remains stable. Thus, the sensor was incubated for 40 min in our assay to allow the sensor to reach peak current saturation.

Influence of Different Lengths of Toehold for Strand-Displacement Reaction. Of particular importance for SDR is the length of the toehold. It is one of the key parameters that affect the thermodynamics and kinetics of SDR. The intermolecular forces between DNA molecules may be complicated due to the presence of LNA base. Thus, it will be helpful to understand the influence of toehold length on the kinetics of SDR.

We changed the length of the mutant-type p53 gene fragment, named TM-4, TM-5, TM-6, TM-7, and TM-8 (Table S1, Supporting Information), and made it equivalent to toehold length varying from 4 to 8 nt. Obviously, the SDR equilibrium time decreased with increasing length of toehold (Figure S2, Supporting Information). With the use of the 7 nt toehold probe, SDR can be completed after 20 min incubation, and it shows the shortest equilibrium time compared with TM-4, TM-5, and TM-6. The possible reason might be that the toehold exchange breaks the coupling between the thermodynamics of the reaction and the kinetics of strand displacement.[34,35] As a result, faster strand displacement reactions are more thermodynamically favorable with the use of longer toehold probe. Interestingly, we found that TM-8 also had an equilibrium time of about 20 min, indicating that a toehold length of 7 nt is the optimal length in our assay. Thus, TM-7 was chosen as the target strand.

Influence of the Longer DNA Targets. To demonstrate that longer DNA strands can also be detected by this DNA sensor, 34-mer and 44-mer oligonucleotides were hybridized onto the DNA sensor. The capture probe was still the 24 nt LNA-integrated sequence used before. Thus, the complementary domain between capture probe and target was 24 nt long and located in the 5′-ends of the target oligonucleotides. The nonhybridized target sequences were oriented into the solution (10 and 20 nt overhang, respectively, see Table S1, Supporting

dx.doi.org/10.1021/ac500362z | Anal. Chem. 2014, 86, 2543−2548

Information; mutant-type target DNA probe TM-34 and 44, Supporting Information). As shown in Figure S3, Supporting Information, the calculated percent changes of ACV signals slightly decreased with increasing target length. The reason might be that the steric hindrance effect of target DNA becomes obvious when extending the length of the DNA sequence. However, it is worth noting that the signal suppression of longer DNA sequences is good enough when compared with that of mismatched DNA. Therefore, the DNA sensor is able to detect a longer DNA strand. It should be mentioned that it provides the potential for detection of a DNA fragment which can be extracted through the DNA amplification protocol, for example, the real-time polymerase chain reaction amplification, in real sample.

Selectivity, Specificity, and Sensitivity of the DNA Sensor. *Selectivity.* Since signal-off sensors are susceptible to false-positive responses if, for example, the DNA is degraded by sample contaminants, it will be meaningful to examine the effect of the contaminant-ridden samples on our DNA sensor.[36,37] The selectivity was assessed by incubating each electrode in human urine, soil, saliva, and beer. As shown in Figure 2, TM-7-free samples of human urine, soil, saliva, and

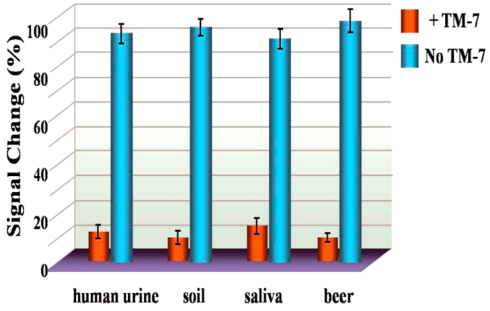

Figure 2. Signal change of different contaminant-ridden samples, in which TM-7 is mixed with human urine, soil solution, saliva, and beer, respectively. Percent change of the peak current $((I_{MB\text{-}L} - I_{MIX})/I_{MB\text{-}L}$, where $I_{MB\text{-}L}$ and I_{MIX} are the peak currents before and after addition of the mixture samples, respectively) of ACV was recorded from three different electrodes.

beer produced no significant change in ACV peak current. When these contaminant-ridden samples were spiked with 100 nM TM-7, the current signal change was similar to that observed in a pure buffer containing 100 nM TM-7. The reason might be that the signal generation in this sensor is based on a target binding-induced conformational change, rather than on nonspecific adsorption.

Specificity. The DNA sensor is capable of discriminating single-base mismatched DNA among abundant perfectly complementary targets and genomic DNA. The DNA sensor is reliable, and we readily detect the target DNA against a 6000-fold (m/m) excess of genomic DNA (Figure 3A). The signal changed by 24.7 ± 2.5% when wild-type DNA was incubated in the genomic DNA and by 76.1 ± 1.3% when target DNA TM-7 was added to the genomic DNA solution. These results demonstrate that the sensor has high specificity, which has no interference in the presence of abundant genomic DNA. In addition, the signal changes of ACV current response to different concentrations of target DNA with and without genomic DNA have been investigated, and the results are presented in Figure 3B. Although the sensor performance in the complicated biological matrixes is slightly inferior to the assay

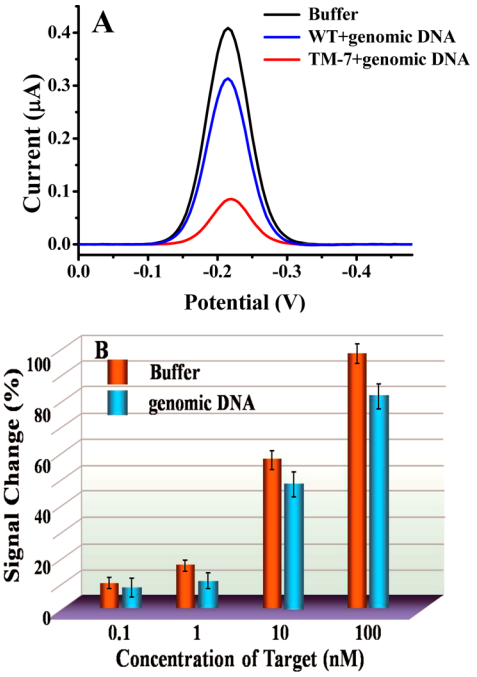

Figure 3. (A) Specificity of DNA sensor is demonstrated in the presence of 6000-fold (m/m) excess denatured herring sperm genomic DNA. (B) Percentage change of ACV current $((I_{MB\text{-}L} - I_{TM\text{-}7})/I_{MB\text{-}L}$, where $I_{MB\text{-}L}$ and $I_{TM\text{-}7}$ are the peak current before and after addition of TM-7, respectively) responses to the various concentrations of TM-7 without (orange bar) and with (blue bar) genomic DNA. All data shown are average measurements from three different electrodes.

in pure target DNA, the DNA sensor provides the potential for detection of target DNA in real samples.

Moreover, the DNA sensor is capable of discriminating between single-base mismatched targets and perfectly complementary DNA. We found that 2% mutant DNA could be detected in the TM-7 and WT mixtures (Figure 4). The results reveal that the DNA sensor is reliable to distinguish mismatched targets from perfect match targets.

To evaluate the interference of different mismatches, we used three different mismatched targets, including mutant A, mutant

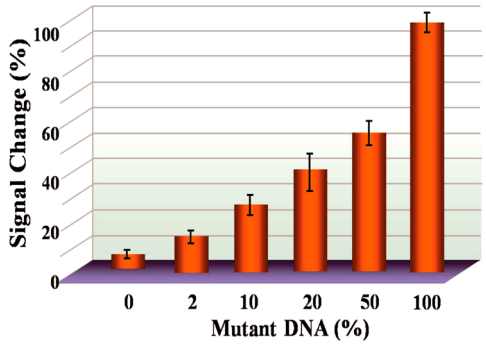

Figure 4. In heterozygous samples, TM-7 and WT are mixed together at various ratios (TM-7/ (WT + TM-7) = 0, 2%, 10%, 20%, 50%, and 100%) with a total concentration of 100 nM. Percent change of the peak current $((I_{MB\text{-}L} - I_{MIX})/I_{MB\text{-}L}$, where $I_{MB\text{-}L}$ and I_{MIX} are the peak currents before and after addition of the DNA mixture, respectively) of ACV increased with increasing percentage of mutant-type DNA in sample solutions. Data shown are average measurements from three different electrodes.

dx.doi.org/10.1021/ac500362z | *Anal. Chem.* 2014, 86, 2543−2548

C, and random DNA sequences (Table S1, Supporting Information). Figure S4, Supporting Information, shows the signal changes from ACV experiments after incubating the DNA sensor with different targets. The ACV response of mutant A and mutant C has much lower signal changes than that of mutant T. In addition, as expected, almost no change of ACV signal is observed for the capture probe hybridized with noncomplementary sequence, since hybridization hardly occurs between the capture and the noncomplementary sequence. These results illustrate that the proposed DNA sensor is able to effectively detect the mutant T DNA with high specificity.

Sensitivity. The sensitivity of this method was evaluated using different concentrations of TM-7 (0, 0.5, 1, 2, 5, 10, 20, 50, 100, and 200 nM). As shown in Figure 5, the signal

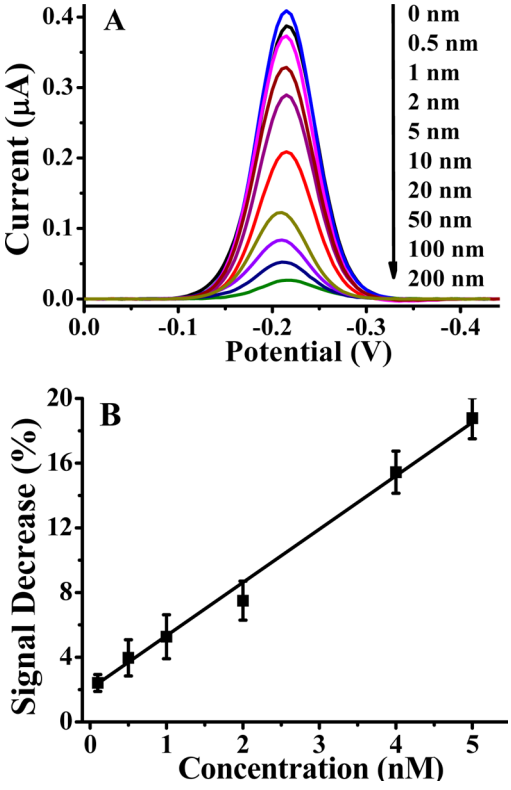

Figure 5. (A) Alternating current voltammograms of the sensor with addition of TM-7 solution at concentrations of 0, 0.5, 1, 2, 5, 10, 20, 50, 100, and 200 nM (from top to buttom). (B) Linear relationship between the signal decrease percentage ($(I_{MB\text{-}L} - I_{TM\text{-}7})/I_{MB\text{-}L}$, where $I_{MB\text{-}L}$ and $I_{TM\text{-}7}$ are the peak current before and after addition of TM-7, respectively) and the concentration of TM-7. All measurements were performed in PB solution (100 mM phosphate, pH 7.4). Data shown are average measurements from three different electrodes.

decreases with increasing concentration of target DNA. The regression equation was expressed as $y = 3.2342x + 2.0614$ (x is the concentration of TM-7, y is the signal decrease percentage). The detection limit, based on 3σ/slope (where σ is the standard deviation), was calculated to be 58 pM with a correlation coefficient R value of 0.9984, which can be detected experimentally (Figure S5, Supporting Information). This approach is much more sensitive than previous methods.[6]

One of the most important reasons for improving SNPs discriminating ability is that the ΔT_m value of LNA/DNA hybrids is much larger than that of DNA/DNA hybrids. This indicates that LNA-integrated strand has much more binding force to target sequence and better recognition ability of single-base mismatches. As shown in Figure S6, Supporting Information, the melting temperature of LNA−DNA perfectly matched duplex (71.1 °C) was higher than that of DNA−DNA perfectly matched duplex (61.5 °C). Moreover, T_m of LNA-DNA mismatched duplex was decreased to 51.2 °C, which was much lower than that of DNA−DNA mismatched duplex (57.4 °C). The ΔT_m value of LNA/DNA hybrids became larger, suggesting that the SDR is much easier to occur when mutant-type DNA is present and the SDR is much harder to occur when wild-type DNA is present. Thus, it is greatly helpful to improve the sensitivity and selectivity in the detection of SNPs.

Regenerability of the DNA Sensor. T-P was covalently attached on gold surface through the Au−S bond, which allowed the sensor to be stable enough to regenerate and establish ON−-OFF switching. As shown in Figure 6A,

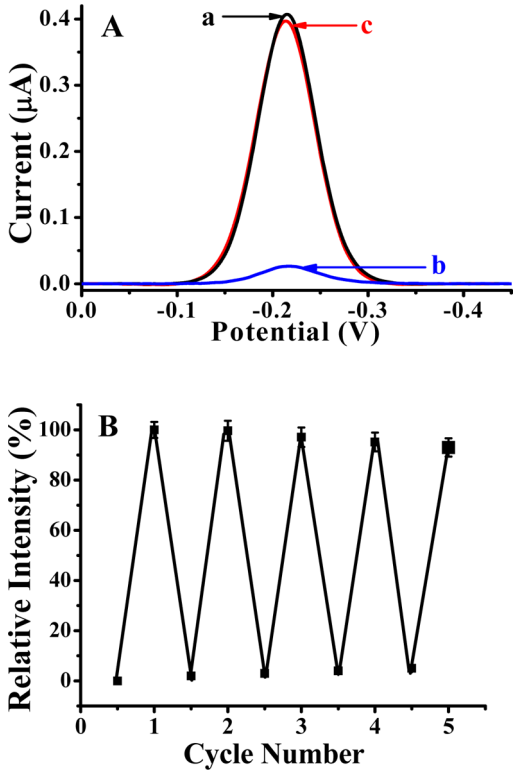

Figure 6. (A) ACV responses of the regenerated sensor. In the presence of MB-L (100 nM), a well-defined peak current is obtained (curve a). When TM-7 was added, the peak current decreased dramatically (curve b). After regeneration, the current recovered 98% of original current (curve c). (B) Reversibility of the sensor over five cycle uses. Relative intensity is calculated with the initial $I_{MB\text{-}L}$ and $I_{TM\text{-}7}$ values as 100% and 0%, respectively. Data shown are average measurements from three different electrodes.

compared with the initial peak current (curve a), the peak current produced a signal suppression of 91.6 ± 1.8% after hybridization between MB-L and TM-7 (curve b) and regenerated 98 ± 2.2% of the original signal successfully (curve c) by immersing the regenerated electrode in the MB-L solution. The sensor could reproducibly detect TM-7 over five tested reuses (Figure 6B). It demonstrates that this DNA sensor has good reversibility. Thus, regeneration is another appealing advantage for the sensing system.

dx.doi.org/10.1021/ac500362z | *Anal. Chem.* 2014, 86, 2543−2548

CONCLUSIONS

We proposed a sensitive ON−OFF switching DNA sensor with high SNPs discrimination ability by employing LNA-integrated and toehold-mediated SDR methods. As a proof-of-concept, this strategy provides an easily regenerated platform, as well as a highly sensitive and selective detection for SNPs. This strategy has several excellent features. First, our method provides an ON−OFF switching sensor, which has the characteristics of easy regeneration and good stability. In this sensing system, the wild-type DNA or mutant-type DNA can be detected by the ON or OFF state. Second, we introduce LNA and SDR techniques into the SNPs sensing system, which improve the detection capability and reaction rate. Third, this sensing system manifests a remarkable discrimination capability of SNPs with high selectivity and specificity toward single-base mismatched DNA among abundant wild-type targets and genomic DNA. This DNA sensor even works in complex, contaminant-ridden samples. Finally, the DNA sensor for detection of SNPs can be fabricated without any kind of enzyme. We may expect this approach to provide an inspiring strategy for SNPs detection and offer the groundwork for the design of other regenerated platforms for biosensing applications, such as detection of metal ions and proteins. Our further research will focus on improvement of the sensitivity and propose a more practical sensor for SNPs analysis in real samples.

ASSOCIATED CONTENT

Supporting Information

Table S1 and Figures S1−S6. DNA sequences, optimal experiments, and UV melting measurements. This material is available free of charge via the Internet at http://pubs.acs.org.

AUTHOR INFORMATION

Corresponding Author

*Phone: +86 23 68253237. Fax: +86 23 68253237. E-mail: linb@swu.edu.cn.

Author Contributions

This manuscript was written through contributions of all authors. All authors have given approval to the final version of the manuscript.

Notes

The authors declare no competing financial interest.

ACKNOWLEDGMENTS

This work was financially supported by the National Natural Science Foundation of China (Nos. 21273174 and 20975083) and the Municipal Science Foundation of Chongqing City (No. CSTC-2013jjB00002).

REFERENCES

(1) Boffa, M. B.; Maret, D.; Hamill, J. D.; Bastajian, N.; Crainich, P.; Jenny, N. S.; Tang, Z. H.; Macy, E. M.; Tracy, R. P.; Franco, R. F.; Nesheim, M. E.; Koschinsky, M. L. *Blood* **2008**, *111*, 183−189.

(2) Brookes, A. J. *Gene* **1999**, *234*, 177−186.

(3) Engle, L. J.; Simpson, C. L.; Landers, J. E. *Oncogene* **2006**, *25*, 1594−1601.

(4) McCarthy, J. J.; Hilfiker, R. *Nat. Biotechnol.* **2000**, *18*, 505−508.

(5) Gao, Z.; Shen, W.; Deng, H.; Ren, Y. *Chem. Commun.* **2013**, *49*, 370−372.

(6) Wang, D. Z.; Tang, W.; Wu, X.; Wang, X.; Chen, G.; Chen, Q.; Li, N.; Liu, F. *Anal. Chem.* **2012**, *84*, 7008−7014.

(7) Ross, P.; Hall, L.; Smirnov, I.; Haff, L. *Nat. Biotechnol.* **1998**, *16*, 1347−1351.

(8) Nie, B.; Shortreed, M. R.; Smith, L. M. *Anal. Chem.* **2005**, *77*, 6594−6600.

(9) Wang, H.; Li, J.; Wang, Y. X.; Jin, J. Y.; Yang, R. H.; Wang, K.; Tan, W. H. *Anal. Chem.* **2010**, *82*, 7684−7690.

(10) Tobe, V. O.; Taylor, S. L.; Nickerson, D. A. *Nucleic Acids Res.* **1996**, *24*, 3728−3732.

(11) Xue, X. J.; Xu, W.; Wang, F.; Liu, X. G. *J. Am. Chem. Soc.* **2009**, *131*, 11668−11669.

(12) Li, J.; Zhong, W. *Anal. Chem.* **2007**, *79*, 9030−9038.

(13) Li, J. S.; Deng, T.; Chu, X.; Yang, R. H.; Jiang, J. H.; Shen, G. L.; Yu, R. Q. *Anal. Chem.* **2010**, *82*, 2811−2816.

(14) Howell, W. M.; Jobs, M.; Gyllensten, U.; Brookes, A. J. *Nat. Biotechnol.* **1999**, *17*, 87−88.

(15) Wei, F.; Chen, C.; Zhai, L.; Zhang, N.; Zhao, X. S. *J. Am. Chem. Soc.* **2005**, *127*, 5306−5307.

(16) Xiao, Y.; Lou, X. H.; Uzawa, T.; Plakos, K. J. I.; Plaxco, K. W.; Soh, H. T. *J. Am. Chem. Soc.* **2009**, *131*, 15311−15316.

(17) Xiao, Y.; Pavlov, V.; Niazov, T.; Dishon, A.; Kotler, M.; Willner, I. *J. Am. Chem. Soc.* **2004**, *126*, 7430−7431.

(18) Zhang, H.; Li, F.; Dever, B.; Li, X. F.; Le, X. C. *Chem. Rev.* **2013**, *113*, 2812−2841.

(19) Xiao, Y.; Piorek, B. D.; Plaxco, K. W.; Heeger, A. J. *J. Am. Chem. Soc.* **2005**, *127*, 17990−17991.

(20) Wang, F.; Elbaz, J.; Willner, I. *J. Am. Chem. Soc.* **2012**, *134*, 5504−5507.

(21) Genot, A. J.; Zhang, D. Y.; Bath, J.; Turberfield, A. J. *J. Am. Chem. Soc.* **2011**, *133*, 2177−2182.

(22) Wang, X.; Zou, M.; Huang, H.; Ren, Y.; Li, L.; Yang, X.; Li, N. *Biosens. Bioelectron.* **2013**, *41*, 569−575.

(23) Zhang, Z.; Zeng, D.; Ma, H.; Feng, G.; Hu, J.; He, L.; Li, C.; Fan, C. *Small* **2010**, *6*, 1854−1858.

(24) Sau, S. P.; Kumar, T. S.; Hrdlicka, P. J. *Org. Biomol. Chem.* **2010**, *8*, 2028−2036.

(25) Østergaard, M. E.; Hrdlicka, P. J. *Chem. Soc. Rev.* **2011**, *40*, 5771−5788.

(26) Iliadi, A.; Petropoulou, M.; Ioannou, P. C.; Christopoulos, T. K.; Anagnostopoulos, N. I.; Kanavakis, E.; Synodinos, J. T. *Anal. Chem.* **2011**, *83*, 6545−6551.

(27) MacAskill, A.; Crawford, D.; Graham, D.; Faulds, K. *Anal. Chem.* **2009**, *81*, 8134−8140.

(28) Mishra, S.; Ghosh, S.; Mukhopadhyay, R. *Langmuir* **2012**, *28*, 4325−4333.

(29) Kaur, H.; Babu, B. R.; Maiti, S. *Chem. Rev.* **2007**, *107*, 4672−4697.

(30) Veedu, R. N.; Wengel, J. *Mol. BioSyst.* **2009**, *5*, 787−792.

(31) Campbell, M. A.; Wengel, J. *Chem. Soc. Rev.* **2011**, *40*, 5680−5689.

(32) Natsume, T.; Ishikawa, Y.; Dedachi, K.; Tsukamoto, T.; Kurita, N. *Chem. Phys. Lett.* **2007**, *446*, 151−158.

(33) Gao, Z. F.; Gao, J. B.; Zhou, L. Y.; Zhang, Y.; Si, J. C.; Luo, H. Q.; Li, N. B. *RSC Adv.* **2013**, *3*, 12334−12340.

(34) Zhang, D. Y.; Winfree, E. *J. Am. Chem. Soc.* **2009**, *131*, 17303−17314.

(35) Zhang, D. Y.; Turberfield, A. J.; Yurke, B.; Winfree, E. *Science* **2007**, *318*, 1121−1125.

(36) Cash, K. J.; Heeger, A. J.; Plaxco, K. W.; Xiao, Y. *Anal. Chem.* **2009**, *81*, 656−661.

(37) Fan, C.; Plaxco, K. W.; Heeger, A. J. *Proc. Natl. Acad. Sci. U.S.A.* **2003**, *100*, 9134−9137.